

speeds (i.e., flight-envelope speeds) at matched loft-ceilings, etc. in a study of a 2-D vertical-plane chase. An account of differential-turn-maneuvering tactics is given in Ref. 9.

References

- ¹Kelley, H. J. and Lefton, L., "Supersonic Aircraft Energy Turns," Fifth IFAC Congress, Paris, France, 1972; also *Automatica*, Vol. 8, Sept. 1972, pp. 575-580.
- ²Kelley, H. J., "Aircraft Maneuver Optimization by Reduced-Order Approximation," in Vol. X of *Control and Dynamic Systems: Advances in Theory and Applications*, edited by C. T. Leondes, Academic Press, New York, 1973.
- ³Kelley, H. J. and Lefton, L., "Differential Turns," *AIAA Journal*, Vol. 11, No. 6, June 1973, pp. 858-861.
- ⁴Falco, M. and Kelley, H. J., "Aircraft Symmetric Flight Optimization," in Vol. X of *Control and Dynamic Systems: Advances in Theory and Applications*, edited by C. T. Leondes, Academic Press, New York, 1973.

vances in Theory and Applications, edited by C. T. Leondes, Academic Press, New York, 1973.

⁵Preys, A. E. and Willes, R. E., "Air Combat Maneuvering," USAF Academy Notes, 1969; also Vol. II of *Advanced Aircraft Propulsion/Engagement Study*, TR 71-7, USAF Academy, Colorado Springs, Colo., Sept. 1971.

⁶Kelley, H. J. and Sullivan, H. C., "Roll-Modulated Lifting Entry Optimization," *AIAA Journal*, Vol. 11, No. 7, July 1973, pp. 913-915.

⁷Contensou, P., "Etude Théorique des Trajectoires dans un Champ de Gravitation. Application au Cas d'un Centre d'Attraction Unique," *Astronautica Acta*, Vol. VIII, Fasc. 2-3, 1962, pp. 134-150.

⁸Boyd, J. R., "Maximum Maneuver Concept," informal briefing, USAF Systems Command Headquarters, Andrews Air Force Base, Md., July 1971; also briefing notes by J. R. Boyd, T. P. Christie, and R. E. Drabant, Eglin Air Force Base, Fla., Aug. 1971.

⁹Kelley, H. J., "Differential Turning Tactics," Paper 74-815, AIAA/AAS Mechanics and Control of Flight Conference, Anaheim, Calif., 1974.

JANUARY 1975

J. AIRCRAFT

VOL. 12, NO. 1

Coordinated Adaptive Washout for Motion Simulators

Russell V. Parrish,* James E. Dieudonne,* Roland L. Bowles*

NASA Langley Research Center, Hampton, Va.

and

Dennis J. Martin Jr.†

Electronic Associates, Inc., Hampton, Va.

This paper introduces a new method of providing motion cues to a moving base six-degree-of-freedom flight simulator utilizing nonlinear filters. Coordinated adaptive filters, used to coordinate translational and rotational motion, are derived based on the method of continuous steepest descent, and the basic concept of the digital controllers used for the uncoordinated heave and yaw cues is also presented. The coordinated adaptive washout method is illustrated by an application in a six-degree-of-freedom fixed-base environment.

Nomenclature

A	= angular position break point, rad
a_x, a_y, a_z	= aircraft body axis translational accelerations, m/sec ²
B	= angular velocity threshold, rad/sec
b_x, b_y	= coefficient for position penalty in cost function, per sec ⁴
C	= angular velocity washout rate, rad/sec ²
c_x, c_y	= coefficient for velocity penalty in cost function, per sec ²
d_x, d_y	= damping parameters for second-order translational washout, rad/sec
e_x, e_y	= frequency parameters for second-order translational washout, rad/sec ²
$f_{l,x}; f_{l,y}; f_{l,z}$	= inertial axis translational acceleration commands, m/sec ²
$f_{s,x}; f_{s,y}$	= body axis longitudinal and lateral acceleration at motion simulator centroid location, m/sec ²
$f_{s,z}$	= body axis vertical acceleration (referenced about lg) at motion simulator centroid location, m/sec ²

g	= gravitational constant, m/sec ²
J_x, J_y	= longitudinal and lateral cost function
K_D	= digital controller gain parameter
$K_{x,1}; K_{x,2}; K_{x,3}$	= longitudinal gain parameters
$K_{y,1}; K_{y,2}; K_{y,3}$	= lateral gain parameters
p, q, r	= body axis angular velocity commands, rad/sec
p_a, q_a, r_a	= body axis aircraft angular velocities, rad/sec
$p_{x,1}; p_{x,2}; p_{x,3}$	= longitudinal adaptive parameters
$p_{y,1}; p_{y,2}; p_{y,3}$	= lateral adaptive parameters
t	= time, sec
t_1, t_2	= arbitrary time, sec
W_x, W_y	= angular rate weighting coefficient, m ⁴ /rad ² sec ²
x, y, z	= commanded inertial translational position of motion simulator, m
ψ, θ, ϕ	= commanded inertial angular position of motion simulator, rad
$\dot{\psi}_a, \dot{\theta}_a, \dot{\phi}_a$	= angular velocity input commands, rad/sec†
τ_1, τ_2	= time when ψ reaches breakpoint, A, sec

I. Introduction

A NEW method of providing motion cues to a moving base six-degree-of-freedom flight simulation has been developed at Langley Research Center. The method, coordinated adaptive washout, is based on the idea of coordination of rotation and translation to obtain accurate longitudinal and lateral force cues in a manner similar to the work of Schmidt and Conrad.^{1,2} The major differences between the subject scheme and the work of Schmidt and

Presented as Paper 73-930 at the AIAA Visual and Motion Simulation Conference, Palo Alto, Calif., September 10-12, 1973; submitted September 19, 1973; revision received July 8, 1974.

Index category: Computer Technology and Computer Simulation Techniques.

*Aero-Space Technologists, Simulation Programming and Analysis Section, Analysis and Simulation Branch, Analysis and Computation Division.

†Programmer-Analyst, Analysis and Programing Department.

†A dot over a variable indicates the time derivative of that variable.

Conrad are that the washout is carried out in the inertial reference frame rather than the body axis system, and employs nonlinear filters rather than the linear filters used by Schmidt and Conrad.

Two types of nonlinear filters, coordinated adaptive filters and digital controllers, have been developed and are employed in the new washout method. The design philosophy for these filters was to present as much of the cue as possible within the constraints of the motion base, without regard to human factors criterion. Coordinated adaptive filters, based on continuous steepest descent, are used for both the longitudinal cues (coordinating surge and pitch) and the lateral cues (coordinating sway and roll). At present, these filters are designed to provide translational specific force cues and rotational rate cues (motivation for the representation of rotational rates rather than rotational accelerations may be found in Ref. 2, page 6). The second type of nonlinear filter, the digital controller, is used to provide the uncoordinated heave and yaw cues. A first-order digital controller provides the yaw-rate cue, while a second-order digital controller provides the vertical specific force cue.

This paper will present the coordinated adaptive washout method, a discussion of the nonlinear filters, an evaluation of the methods, and an illustration of an application in a six-degree-of-freedom environment.

II. Coordinated Adaptive Washout

The washout circuitry is illustrated in block diagram form in Fig. 1. Assuming that it is desired to create in the body axis of the motion base the same motion situation present in the body axis of the simulated aircraft (ignoring for the moment the base constraints), the body axis translational accelerations and rotational rates of the aircraft are transformed into the inertial axis system of the motion base through the Euler angles of the base. The resulting inertial specific forces and Euler rates are then available for washout by the nonlinear filters. As shown in the diagram, coordinated adaptive filters are used for both the longitudinal cues (coordinating surge and pitch) and the lateral cues (coordinating sway and roll). A first-order digital controller is used to provide yaw-rate washout, and a second-order digital controller provides the heave cue.

Transformation of the washed-out translational acceleration and rotational rates back into the body axis of the motion base is then provided in order to compare the washout commands to the aircraft motions. The comparison is presented in real time in the form of the time history overlays on a cathode ray tube.³ Overlays of the inertial situation are also available.

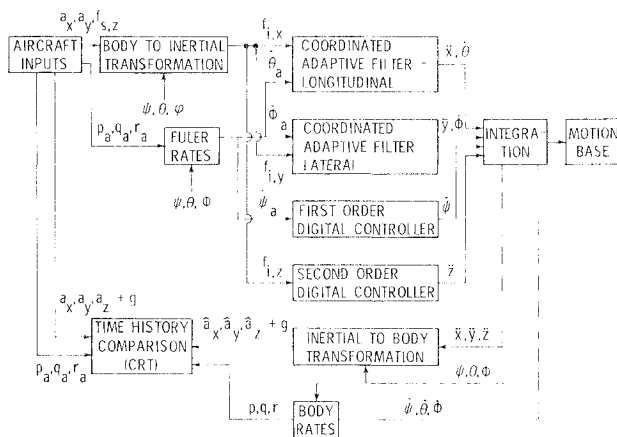


Fig. 1 Coordinated adaptive washout circuit.

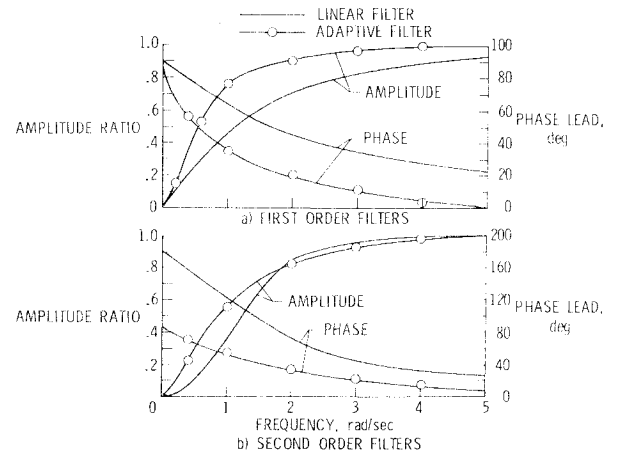


Fig. 2 Frequency response comparison of linear and adaptive filters.

Coordinated Adaptive Filters

The adaptive filter used to coordinate both surge-pitch and sway-roll was originally derived as an adaptive filter for single-degree-of-freedom application. Figure 2 presents a comparison of amplitude ratio and phase lead of this nonlinear adaptive filter and a linear filter for the same motion base constraints over the frequency range of interest. The comparison is presented for both the first- and second-order single-degree-of-freedom case, and since the amplitude and phase response of the nonlinear adaptive filter changes with the magnitude of the input, the worst case comparison for the nonlinear filter, that of maximum input amplitude, is presented. As can be seen, the steady-state amplitude and phase response of the adaptive filter is better than that of the linear filter for both cases.

The extension of the adaptive filter to a coordinated adaptive filter is presented in Ref. 4. In this extension, the two-degree-of-freedom small angle approximation case was treated. The present paper will further extend the adaptive filter to the six-degree-of-freedom environment, beginning with the full derivation of the longitudinal filter and then a brief derivation of the lateral filter.

Longitudinal Filter

Given the longitudinal specific force in the inertial axis system of the motion base, $f_{i,x}$, to be

$$f_{i,x} = \ddot{x}_a (\cos \theta \cos \psi) + \ddot{y}_a (\sin \phi \sin \theta \cos \psi - \cos \phi \sin \psi) + (\ddot{z}_a - g)(\cos \phi \sin \theta \cos \psi + \sin \phi \sin \theta) \quad (1)$$

where

$$f_{s,z} = \ddot{a}_z + g$$

define a cost function, J_x , as

$$J_x = \frac{1}{2} (f_{i,x} - \ddot{x})^2 + \frac{W_x}{2} (\dot{\theta}_a - \dot{\theta})^2 + \frac{b_x}{2} \dot{x}^2 + \frac{c_x}{2} \ddot{x}^2 \quad (2)$$

Define the control laws (the adaptive filters) as

$$\ddot{x} = p_{x,1} f_{i,x} - d_x \dot{x} - c_x x \quad (3)$$

$$\dot{\theta} = p_{x,2} f_{i,x} + p_{x,3} \dot{\theta}_a \quad (4)$$

$p_{x,j}$ ($j = 1, 2, 3$) are adaptive parameters. Applying continuous steepest descent⁵ yields

$$\dot{p}_{x,j} = -K_{x,j} \frac{\partial J_x}{\partial p_{x,j}} \quad (5)$$

$j = 1, 2, 3$

$$\frac{\partial f_{i,x}}{\partial p_{x,j}} = (f_{i,x} - \ddot{x}) \left(\frac{\partial f_{i,x}}{\partial p_{x,j}} - \frac{\partial \ddot{x}}{\partial p_{x,j}} \right) - W_x(\dot{\theta}_a - \dot{\theta}) \frac{\partial \dot{\theta}}{\partial p_{x,j}} + b_x \dot{x} \frac{\partial x}{\partial p_{x,j}} + c_x \dot{x} \frac{\partial \dot{x}}{\partial p_{x,j}} \quad (6)$$

$$\dot{p}_{x,j} = K_{x,j} \left\{ (f_{i,x} - \ddot{x}) \left(\frac{\partial \ddot{x}}{\partial p_{x,j}} - \frac{\partial f_{i,x}}{\partial p_{x,j}} \right) + W_x(\theta_a - \dot{\theta}) \frac{\partial \dot{\theta}}{\partial p_{x,j}} - b_x \dot{x} \frac{\partial x}{\partial p_{x,j}} - c_x \dot{x} \frac{\partial \dot{x}}{\partial p_{x,j}} \right\} \quad (7)$$

The state sensitivity equations are obtained by assuming that the parameters are independent, and that the derivatives are continuous in the adaptive parameters and time,^{5,6} such that

$$\frac{\partial}{\partial p} \left(\frac{d^2 x}{dt^2} \right) = \frac{d^2}{dt^2} \left(\frac{\partial x}{\partial p} \right) = \left(\frac{\partial \dot{x}}{\partial p} \right)$$

Thus

$$\left(\frac{\partial \dot{x}}{\partial p_{x,j}} \right) = \frac{\partial p_{x,1} f_{i,x}}{\partial p_{x,j}} + p_{x,1} \frac{\partial f_{i,x}}{\partial p_{x,j}} - d_x \left(\frac{\partial \dot{x}}{\partial p_{x,j}} \right) - e_x \frac{\partial x}{\partial p_{x,j}} \quad (8)$$

$$\left(\frac{\partial \dot{\theta}}{\partial p_{x,j}} \right) = \frac{\partial p_{x,2} f_{i,x}}{\partial p_{x,j}} + p_{x,2} \frac{\partial f_{i,x}}{\partial p_{x,j}} + \frac{\partial p_{x,3} \dot{\theta}_a}{\partial p_{x,j}} \quad (9)$$

Finally,

$$\frac{\partial f_{i,x}}{\partial p_{x,j}} = [-a_x(\sin \theta \cos \psi) + a_y(\sin \phi \cos \theta \cos \psi) + (f_{s,z} - g)(\cos \phi \cos \theta \cos \psi)] \frac{\partial \theta}{\partial p_{x,j}} \quad (10)$$

assuming

$$\frac{\partial \phi}{\partial p_{x,j}} = \frac{\partial \psi}{\partial p_{x,j}} = 0.$$

Expansion of Eq. (9) for $j = 1$ yields

$$\begin{aligned} \left(\frac{\partial \dot{\theta}}{\partial p_{x,1}} \right) &= p_{x,2} \frac{\partial f_{i,x}}{\partial p_{x,1}} \\ &= p_{x,2} [-a_x(\sin \theta \cos \psi) + a_y(\sin \phi \cos \theta \cos \psi) \\ &\quad + (f_{s,z} - g)(\cos \phi \cos \theta \cos \psi)] \frac{\partial \theta}{\partial p_{x,1}} \end{aligned}$$

However, since $\partial \theta / \partial p_{x,1}(0) = 0$, then $\partial \dot{\theta} / \partial p_{x,1}(t) = 0$, which implies

$$\frac{\partial \theta}{\partial p_{x,1}}(t) = 0 \text{ and } \frac{\partial f_{i,x}}{\partial p_{x,1}} = 0$$

Simultaneous integration in real time of these five first-order Eqs. [(7), $j = 1, 2, 3$; (9), $j = 2, 3$] and three second-order Eqs. [(8), $j = 1, 2, 3$] yields the adaptive parameters $p_{x,1}$, $p_{x,2}$, and $p_{x,3}$ used in the control laws, or adaptive filters. Selection of the values of the washout constants $[W_x, b_x, c_x, d_x, e_x, K_{x,j}]$ and $p_{x,j}(0)$, $j = 1, 2, 3$ must, of course, be based on the constraints of the motion base and the flight environment, as well as the desired emphasis of the washout (i.e., to represent specific force, rotational rate, or some combination of both).

Coordination Analysis

With the completed derivation of the longitudinal filter, it is now possible to examine the coordination aspects of the filter design. However, the analysis is greatly simplified in the two-degree-of-freedom small angles approximation case. Therefore, for the purposes of discussion, assume $a_y = f_{s,z} = 0$ and that small angle approximations are valid.

Then

$$f_{i,x} = a_x - g\theta$$

and

$$\ddot{x} = p_{x,1}(a_x - g\theta) - d_x \dot{x} - e_x x \quad (11)$$

$$\dot{\theta} = p_{x,2}(a_x - g\theta) + p_{x,3} \dot{\theta}_a \quad (12)$$

For the case of a sustained forward acceleration, $+a_x$, the translational channel is coordinated with the pitch channel in that the translational channel presents the onset of the cue until the pitch channel has time to align the gravity vector to present the sustained portion of the cue (θ operates to null $a_x - g\theta$, the drive signal of \ddot{x}).

For the case of a positive pitch rate, $+\dot{\theta}_a$, accompanied by no acceleration change, $a_x = 0$, the $g\theta$ term in Eq. (11) induces a negative specific force via translation to offset the positive false cue created by the temporary misalignment of the gravity vector during the pitch-rate cue presentation.

Lateral Filter

As the derivation of the lateral filter follows the same pattern as that of the longitudinal filter, only the equations are presented.

$$\begin{aligned} f_{i,y} &= a_x(\cos \theta \sin \psi) + a_y(\sin \phi \sin \theta \sin \psi \\ &\quad + \cos \phi \cos \psi) \\ &\quad + (f_{s,z} - g)(\cos \phi \sin \theta \sin \psi - \sin \phi \cos \psi) \end{aligned}$$

Cost Function

$$J_y = \frac{1}{2}(f_{i,y} - \ddot{y})^2 + \frac{W_y}{2}(\dot{\phi}_a - \dot{\phi})^2 + \frac{b_y}{2}y^2 + \frac{c_y}{2}\dot{y}^2$$

Control Laws

$$\begin{aligned} \ddot{y} &= p_{y,1}f_{i,y} - d_y \dot{y} - e_y y \\ \dot{\phi} &= -p_{y,2}f_{i,y} + p_{y,3}\dot{\phi}_a \end{aligned}$$

Adaptive Parameter Rates

$$\begin{aligned} \dot{p}_{y,j} &= K_{y,j} \left\{ (f_{i,y} - \ddot{y}) \left(\frac{\partial \ddot{y}}{\partial p_{y,j}} - \frac{\partial f_{i,y}}{\partial p_{y,j}} \right) \right. \\ &\quad \left. + W_y(\dot{\phi}_a - \dot{\phi}) \frac{\partial \dot{\phi}}{\partial p_{y,j}} - b_y \dot{y} \frac{\partial y}{\partial p_{y,j}} - c_y \dot{y} \frac{\partial \dot{y}}{\partial p_{y,j}} \right\}, \quad j = 1, 2, 3 \end{aligned}$$

State Sensitivity Equations

$$\begin{aligned} \left(\frac{\partial \ddot{y}}{\partial p_{y,j}} \right) &= \frac{\partial p_{y,1} f_{i,y}}{\partial p_{y,j}} + p_{y,1} \frac{\partial f_{i,y}}{\partial p_{y,j}} - d_y \left(\frac{\partial \dot{y}}{\partial p_{y,j}} \right) \\ &\quad - e_y \frac{\partial y}{\partial p_{y,j}}, \quad j = 1, 2, 3 \end{aligned}$$

$$\left(\frac{\partial \dot{\phi}}{\partial p_{y,j}} \right) = -\frac{\partial p_{y,2} f_{i,y}}{\partial p_{y,j}} - p_{y,2} \frac{\partial f_{i,y}}{\partial p_{y,j}} + \frac{\partial p_{y,3} \dot{\phi}_a}{\partial p_{y,j}}, \quad j = 2, 3$$

$$\left(\frac{\partial \dot{\phi}}{\partial p_{y,1}} \right) = \frac{\partial \phi}{\partial p_{y,1}} = \frac{\partial f_{i,y}}{\partial p_{y,1}} = 0$$

$$\frac{\partial f_{i,y}}{\partial p_{y,j}} = [a_y(\cos \phi \sin \theta \sin \psi - \sin \phi \cos \psi) - (f_{s,z} - g)$$

$$(\sin \phi \sin \theta \sin \psi + \cos \phi \cos \psi)] \frac{\partial \theta}{\partial p_{y,j}}, \quad j = 2, 3$$

Digital Controller

The two remaining degrees of freedom, yaw and heave, are represented without coordination by use of the second type of nonlinear filter, the digital controller. This filter is

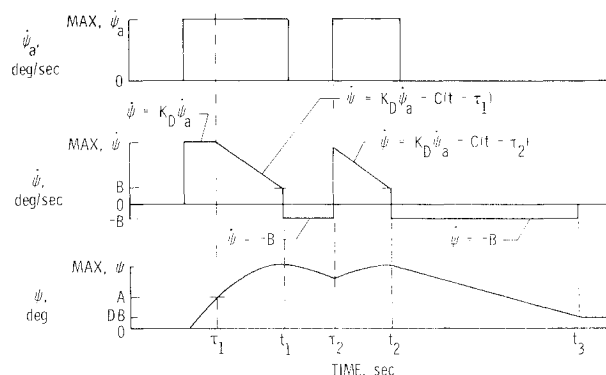


Fig. 3 The design concept of a first-order digital controller.

designed to provide as much of the onset cue as possible before inducing washout through logical switches. Figure 3 illustrates the design concept of the first-order digital controller. From time 0 to τ_1 , a scaled version of the input is commanded. From time τ_1 to t_1 , a linear decay is applied to reduce the command to the threshold value, B . Washout then occurs at the threshold value unless a new input is received (i.e., τ_2).

$$A = \max(\psi) - \left[\frac{\max^2(\psi) - B^2}{2C} \right]$$

$$K_D = \{(2C[\max(\psi) - \psi(\tau_2)] + B^2)^{1/2} / \max(\dot{\psi}_a)\}$$

The design concept of the second-order digital controller is quite similar, although the mechanization is more complex. Figure 4 shows the amplitude and phase versus frequency plots of a linear filter, an adaptive filter, and a digital controller for the same motion base constraints. Both first- and second-order digital controllers show improved response characteristics compared to the linear and adaptive filters. As with Fig. 2, the worst case comparison, that of maximum input, is presented. The servo characteristics of the simulator tend to remove the discontinuities induced by the logical switching of the digital controllers. For study purposes, the dynamics of the simulator were represented by second-order low pass filters⁷ which were fed the output of the digital controllers.

III. Evaluation

In order to evaluate the washout circuitry, it is necessary to choose a motion base to which the circuitry is to be applied. Naturally enough, the Visual Motion Simula-

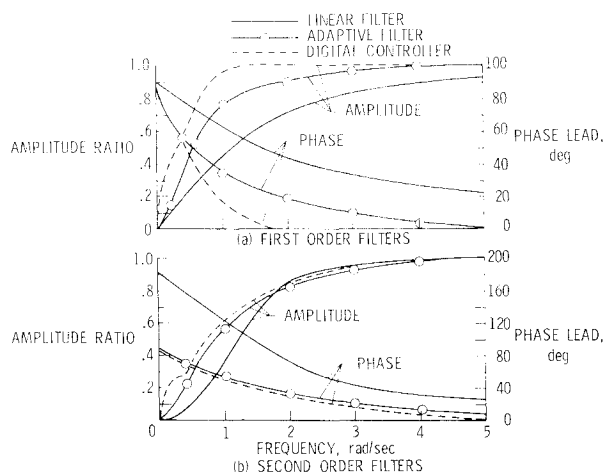
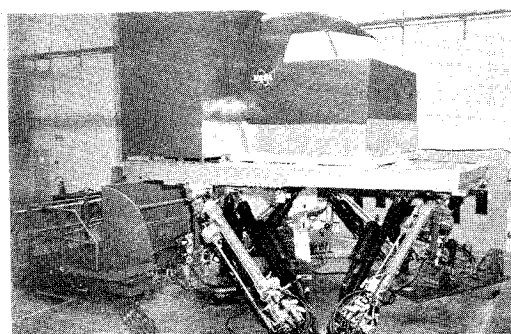


Fig. 4 Frequency response comparison of the three types of filters.



	POSITION	VELOCITY	ACCELERATION
PITCH	+30, -20°	±15°/sec	±50°/sec ²
ROLL	±22°	±15°/sec	±50°/sec ²
YAW	±32°	±15°/sec	±50°/sec ²
VERTICAL	+0.762, -0.991m	±0.610m/sec	±0.6g
LATERAL	±1.219m	±0.610m/sec	±0.6g
LONGITUDINAL	+1.245, -1.219m	±0.610m/sec	±0.6g

Fig. 5 The visual-motion simulator.

tor of Langley Research Center has been chosen for this evaluation.⁷⁻⁹ Figure 5 shows a picture of the simulator and also presents the constraints of the base in each degree of freedom. These constraints are presented for motion in a single degree of freedom. However, due to the synergistic nature of this base, motion in one degree of freedom changes the position limits that may be obtained in each of the other five degrees of freedom. For example, with 10° of pitch, vertical travel is reduced to about ±0.7 meter.

The chronology of the subject washout has not advanced to the point of validation in a flight simulator utilizing the subjective opinions of pilots in the simulated flight environment. Rather, the feasibility of the approach has been evaluated open loop; that is, taped data from a fixed-base flight simulator have been used to drive the washout circuitry. The evaluation phase has consisted of comparing the resulting motion commands with the aircraft specific forces and rotational rates.

Inertial vs Body Comparisons

Figure 6 displays the results of driving the circuitry with flight data obtained from a fixed-base simulation of a jet transport (DC8-707 class). The simulated flight data consist of an elevator doublet, an aileron doublet, and a rudder doublet applied in sequence while flying straight and level. The comparison of aircraft specific forces and rotational rates to washout commands is presented in the inertial axis system. Examination of each degree of freedom reveals that the coordinated adaptive filters have been adjusted to present good specific force cues, $f_{i,x}$ and $f_{i,y}$, at the expense of the rotational cues (note that the coordination burden is heavier for sway and roll than for surge and pitch).⁴ The second-order digital controller is unable to present much of a heave cue in the 0.5-m available travel for this case, while the first-order digital controller has no trouble at all in presenting the low magnitude yaw-rate cue.

Examination of the same results presented in the body axis system in Fig. 7 reveals a different picture, however. The fidelity of the surge cue in the body axis at $t \sim 23$ sec is poor. Thus the contrast between inertial axis and body axis comparisons is illustrated. Body axis comparisons present the combined effects of all degrees of freedom on the individual cue. For example, $f_{s,x}$, the surge body axis cue is made up mainly of a sustained pitch angle that is coordinated with fore and aft translation, and also the vertical component.

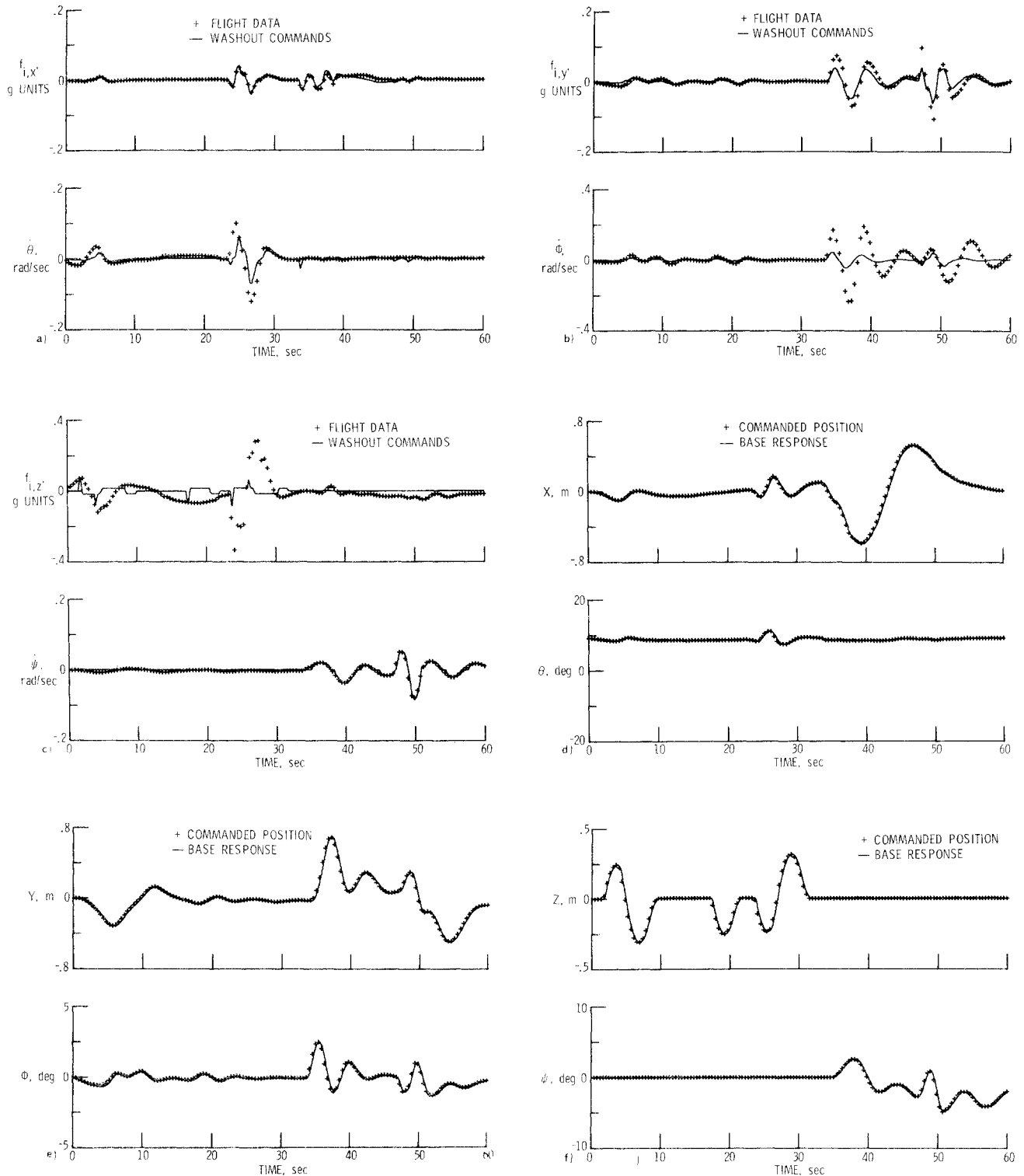


Fig. 6 Washout comparison to flight data in the inertial axis system.

Since so little vertical travel is available with this particular base, examination of this restriction on the surge cue presentation was suggested. Figure 8 displays the longitudinal results of assuming infinite travel in the inertial vertical channel. No changes were made in the washout circuitry for the other five channels. The data are presented in the body axis system, as will be all subsequent data. Fidelity of $f_{s,x}$ is now excellent.

Modification of the Washout

Because of the vertical travel limits of the motion base, presentation of a good heave cue is impossible. However, poor presentation of the heave cue degrades the presentation of the surge cue for the subject washout circuitry. In order to lessen the impact of the vertical travel restriction on the washout operation, the following modification was made to the circuitry in regard to the body to inertial

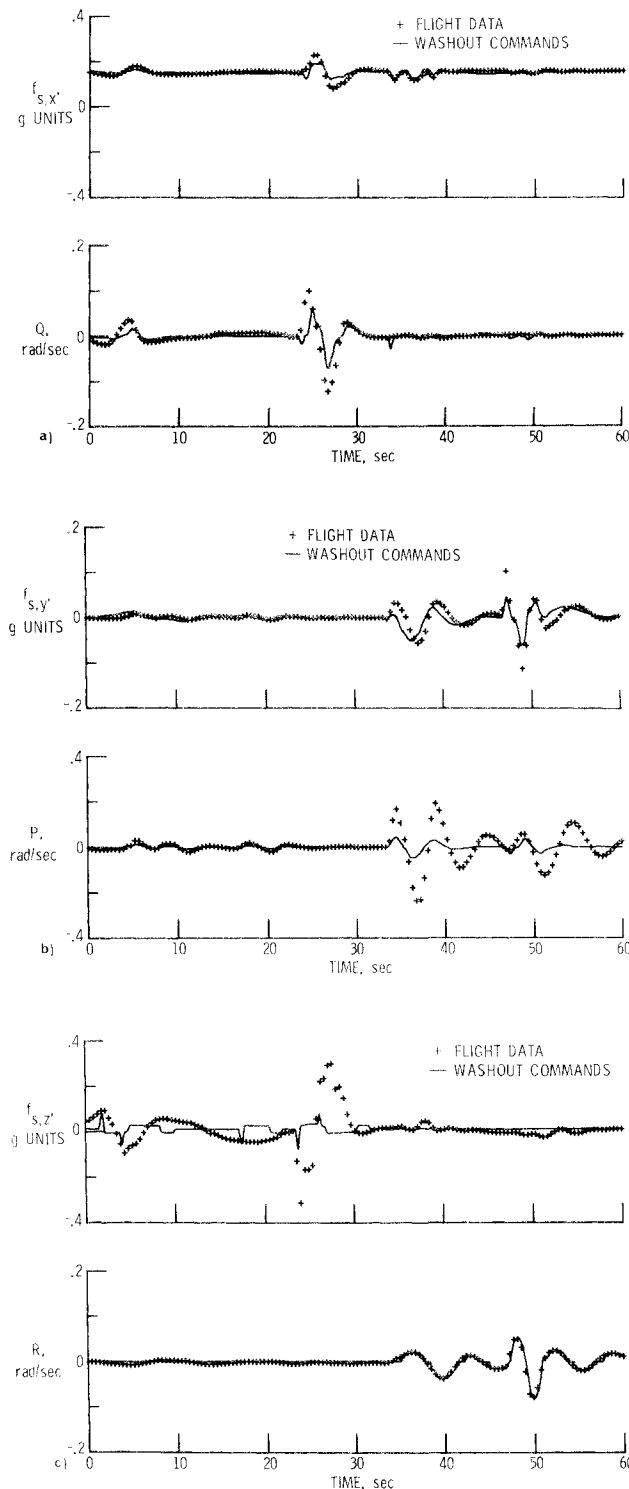


Fig. 7 Washout comparison to flight data in the body axis system.

transformation. The inertial surge and sway required to contribute to the body axis heave would not be represented. Thus

$$\begin{aligned}
 f_{i,x} &= a_x(\cos \theta \cos \psi) + a_y(\sin \phi \sin \theta \cos \psi \\
 &\quad - \cos \phi \sin \psi) - g(\cos \phi \sin \theta \cos \psi + \sin \phi \sin \psi) \\
 f_{i,y} &= a_x(\cos \theta \sin \psi) + a_y(\sin \phi \sin \theta \sin \psi \\
 &\quad + \cos \phi \cos \psi) - g(\cos \phi \sin \theta \sin \psi - \sin \phi \cos \psi)
 \end{aligned}$$

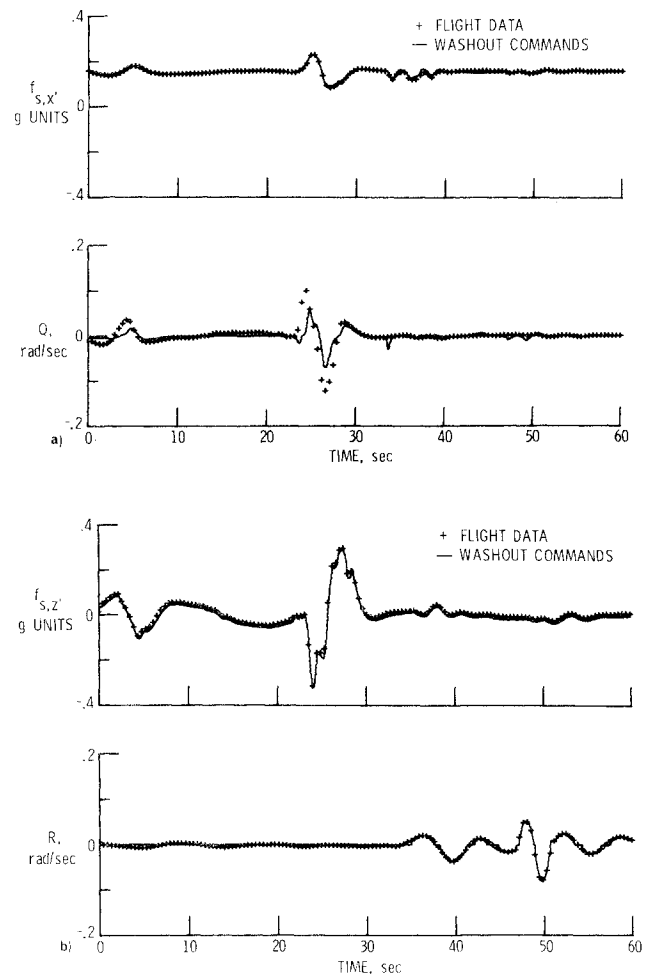


Fig. 8 Body axis longitudinal results for infinite vertical travel.

$$\begin{aligned}
 f_{i,z} &= -a_x(\sin \theta) + a_y(\sin \phi \cos \theta) \\
 &\quad + (f_{s,z} - g)(\cos \phi \cos \theta)
 \end{aligned}$$

The results presented in Fig. 9 illustrate the use of this modification. No other changes have been made in the washout circuitry or parameters, and the second-order digital controller is again being used to present the heave cue. Comparison of Fig. 9 with Fig. 7 shows that the modification of the circuitry has improved the fidelity of the pitch-rate cue, as well as the fidelity of the surge cue. No degradation of the heave cue is noticeable.

IV. Conclusions

Validation of the modified coordinated adaptive washout will be carried out utilizing a moving-base simulation of a 737 jet transport at Langley Research Center in the near future. Further extension of the method to represent rotational accelerations rather than rotational rates is also to be examined.

References

- 1Schmidt, S. F. and Conrad, B., "Motion Drive Signals for Piloted Flight Simulators," Contract NAS2-4869, May 1970, Analytical Mechanics Associates, Inc.; also CR-1601, Palo Alto, Calif., May, 1970, NASA.

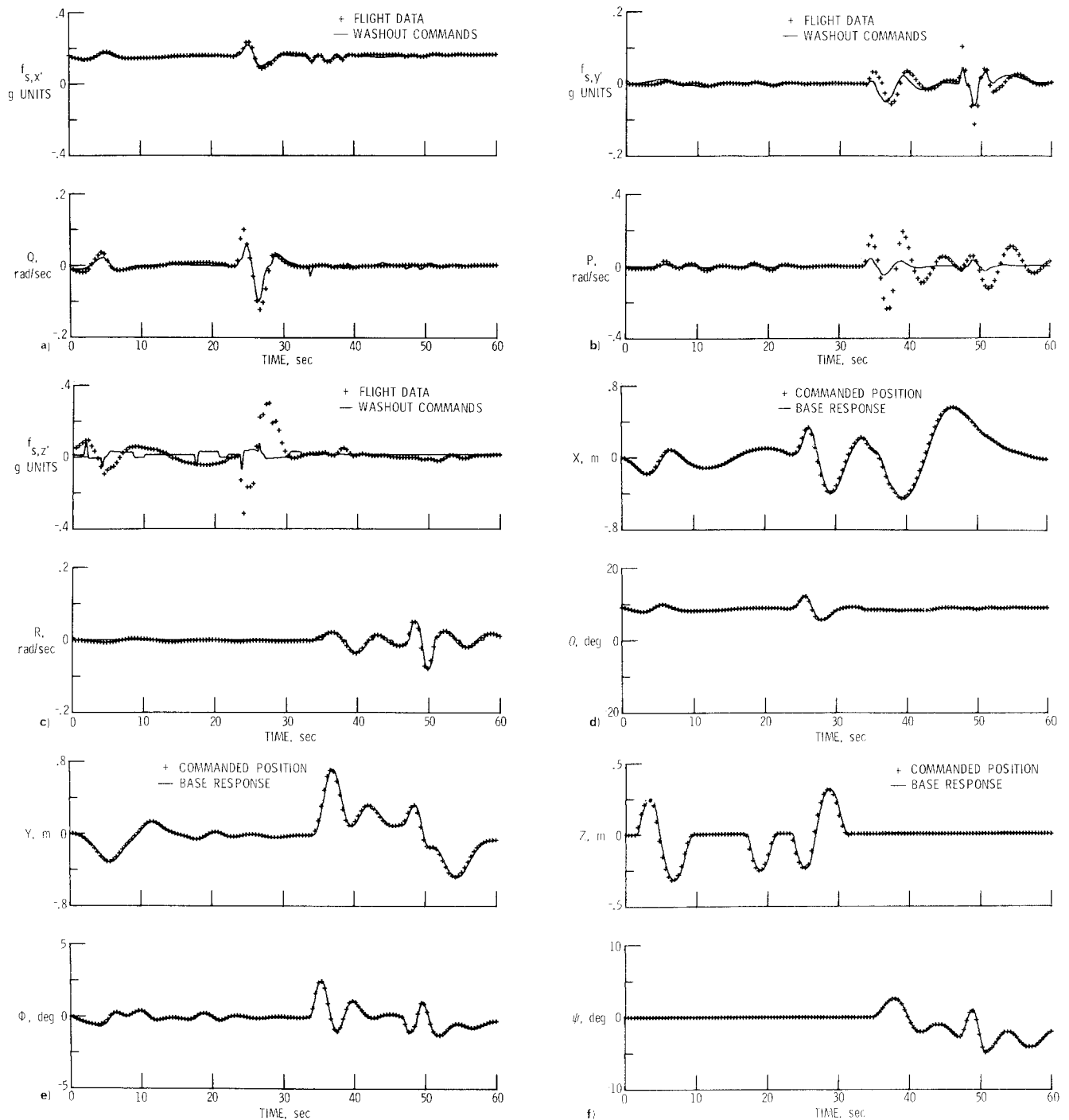


Fig. 9 Modified washout comparison to flight data in the body axis system.

²Schmidt, S. F. and Conrad, B., "A Study of Techniques for Calculating Motion Drive Signals for Flight Simulators," Contract NAS2-5816, July 1971, Analytical Mechanics Associates, Inc.; also CR-114345, Mountain View, Calif., July, 1971, NASA.

³Grove, R. and Mayhew, S. C., "A Real-Time Digital Program for Estimating Stability and Control Parameters From Flight Test Data by Using the Maximum Likelihood Method," TM X-2788 (u), Dec., 1973, NASA.

⁴Parrish, R. V., Dieudonne, J. E., Martin, D. J., Jr., and Bowles, R. L., "Coordinated Adaptive Filters for Motion Simulators," *Proceedings of the 1973 Summer Computer Simulation Conference*, AICHE, ISA, SHARE, SCI, AMS, Vol. 1, pp. 295-300.

⁵Bekey, G. A. and Karplus, J., *Hybrid Computation*, Wiley, New York, 1968.

⁶Coddington, E. A. and Levinson, N. *Theory of Ordinary Differential Equations*, McGraw-Hill, New York, 1955.

⁷Parrish, R. V., Dieudonne, J. E., Martin, D. J. Jr., and Cope-land, J. L., "Compensation Based on Linearized Analysis for a Six-Degree-of-Freedom Motion Simulator," TN D-7349, Nov., 1973, NASA.

⁸Parrish, R. V., Dieudonne, J. E., and Martin, D. J. Jr., "Motion Software for a Synergistic Six-Degree-of-Freedom Motion Base," TN D-7350, Dec., 1973, NASA.

⁹Dieudonne, J. E., Parrish, R. V., and Bardusch, R. E., "An Actuator Extension Transformation for a Motion Simulator and an Inverse Transformation Applying Newton-Raphson's Method," TN D-7067, Nov., 1972, NASA.